



Multi-format signal generation using a frequency-tunable optoelectronic oscillator

YANG CHEN,^{1,3} SHIFENG LIU,² AND SHILONG PAN^{2,4}

¹*School of Information Science and Technology, East China Normal University, Shanghai 200241, China*

²*Key Laboratory of Radar Imaging and Microwave Photonics, Ministry of Education, Nanjing University of Aeronautics and Astronautics, Nanjing 210016, China*

³*ychen@ce.ecnu.edu.cn*

⁴*pans@nuaa.edu.cn*

Abstract: A novel photonic approach for multi-format signal generation based on a frequency-tunable optoelectronic oscillator (OEO) is proposed using a dual-polarization quadrature phase shift-keying (DP-QPSK) modulator. The upper dual-parallel Mach-Zehnder modulator (DP-MZM) integrated in the DP-QPSK modulator is properly biased to serve as an equivalent phase modulator, which functions in conjunction with a phase-shifted fiber Bragg grating (PS-FBG) in the OEO loop as a high-Q microwave photonic band-pass filter. The lower DP-MZM in the DP-QPSK modulator injected by the oscillation signal functions as a frequency multiplier, a phase-coded microwave signal generator or an optical frequency comb generator, respectively, with different signal injection methods. An experiment is performed. When the lower DP-MZM serves as a frequency multiplier, tunable frequency-doubled and quadrupled microwave signals up to 40 GHz are generated without using an optical notch filter; and if it functions as a phase-coded microwave signal generator, fundamental and frequency-doubled binary phase-coded microwave signals are generated with a tunable frequency. Furthermore, tunable five-line optical frequency combs are also generated using the compact system without an external RF source. The performance of the generated signals is also investigated.

© 2018 Optical Society of America under the terms of the [OSA Open Access Publishing Agreement](#)

OCIS codes: (060.5625) Radio frequency photonics; (060.5060) Phase modulation; (350.4010) Microwaves; (280.5600) Radar; (060.4080) Modulation.

References and links

1. J. Capmany and D. Novak, "Microwave photonics combines two worlds," *Nat. Photonics* **1**(6), 319–330 (2007).
2. D. Marpaung, C. Roeloffzen, R. Heideman, A. Leinse, S. Sales, and J. Capmany, "Integrated microwave photonics," *Laser Photonics Rev.* **7**(4), 506–538 (2013).
3. A. Seeds, "Microwave photonics," *IEEE Trans. Microw. Theory Tech.* **50**(3), 877–887 (2002).
4. J. Yao, "Microwave photonics," *J. Lightwave Technol.* **27**(3), 314–335 (2009).
5. S. Pan and J. Yao, "Photonics-based broadband microwave measurement," *J. Lightwave Technol.* **35**(16), 3498–3513 (2017).
6. R. Steed, L. Ponnampalam, M. Fice, C. Renaud, D. Rogers, D. Moodie, G. Maxwell, I. Lealman, M. Robertson, L. Pavlovic, L. Naglic, M. Vidmar, and A. Seeds, "Hybrid integrated optical phase-lock loops for photonic terahertz sources," *IEEE J. Sel. Top. Quantum Electron.* **17**(1), 210–217 (2011).
7. S. Pan, Z. Tang, D. Zhu, D. Ben, and J. Yao, "Injection-locked fiber laser for tunable millimeter-wave generation," *Opt. Lett.* **36**(24), 4722–4724 (2011).
8. L. A. Johansson and A. J. Seeds, "Generation and transmission of millimeter-wave data-modulated optical signals using an optical injection phase-lock loop," *J. Lightwave Technol.* **21**(2), 511–520 (2003).
9. T. Schneider, D. Hannover, and M. Junker, "Investigation of Brillouin scattering in optical fibers for the generation of millimeter waves," *J. Lightwave Technol.* **24**(1), 295–304 (2006).
10. J. Yu, Z. Jia, L. Yi, Y. Su, G. Chang, and T. Wang, "Optical millimeter-wave generation or up-conversion using external modulators," *IEEE Photonics Technol. Lett.* **18**(1), 265–267 (2006).
11. P. Hedekvist, B. Olsson, and A. Wiberg, "Microwave harmonic frequency generation utilizing the properties of an optical phase modulator," *J. Lightwave Technol.* **22**(3), 882–886 (2004).
12. Y. Chen, A. Wen, and L. Shang, "Analysis of an optical mm-wave generation scheme with frequency octupling using two cascaded Mach-Zehnder modulators," *Opt. Commun.* **283**(24), 4933–4941 (2010).

13. H. Chi and J. Yao, "Frequency quadrupling and upconversion in a radio over fiber link," *J. Lightwave Technol.* **26**(15), 2706–2711 (2008).
14. M. Mohamed, X. Zhang, B. Hraimel, and K. Wu, "Frequency sixupler for millimeter-wave over fiber systems," *Opt. Express* **16**(14), 10141–10151 (2008).
15. H. Chi and J. Yao, "Frequency quadrupling and upconversion in a radio over fiber link," *J. Lightwave Technol.* **26**(15), 2706–2711 (2008).
16. X. S. Yao and L. Maleki, "Converting light into spectrally pure microwave oscillation," *Opt. Lett.* **21**(7), 483–485 (1996).
17. S. Pan and J. P. Yao, "A frequency-doubling optoelectronic oscillator using a polarization modulator," *IEEE Photon. Technol. Lett.* **21**(13), 929–931 (2009).
18. D. Zhu, S. Pan, and D. Ben, "Tunable frequency-quadrupling dual-loop optoelectronic oscillator," *IEEE Photon. Technol. Lett.* **24**(3), 194–196 (2012).
19. Y. Chen, W. Li, A. Wen, and J. Yao, "Frequency-Multiplying Optoelectronic Oscillator With a Tunable Multiplication Factor," *IEEE Trans. Microw. Theory Tech.* **61**(9), 3479–3485 (2013).
20. M. Cohen, "Pulse compression in radar systems," in *Principles of Modern Radar*, J. Eaves and E. Reedy (Springer US, 1987).
21. P. Ghelfi, F. Laghezza, F. Scotti, G. Serafino, A. Capria, S. Pinna, D. Onori, C. Porzi, M. Scaffardi, A. Malacarne, V. Vercesi, E. Lazzeri, F. Berizzi, and A. Bogoni, "A fully photonics-based coherent radar system," *Nature* **507**(7492), 341–345 (2014).
22. J. D. McKinney, D. E. Leaird, and A. M. Weiner, "Millimeter-wave arbitrary waveform generation with a direct space-to-time pulse shaper," *Opt. Lett.* **27**(15), 1345–1347 (2002).
23. A. Weiner, "Ultrafast optical pulse shaping: A tutorial review," *Opt. Commun.* **284**(15), 3669–3692 (2011).
24. Y. Chen, A. Wen, and J. Yao, "Photonic generation of frequency tunable binary phase-coded microwave waveforms," *IEEE Photonics Technol. Lett.* **25**(23), 2319–2322 (2013).
25. W. Li, L. Wang, M. Li, H. Wang, and N. Zhu, "Photonic generation of binary phase-coded microwave signals with large frequency tunability using a dual-parallel Mach-Zehnder modulator," *IEEE Photon. J.* **5**(4), 5501507 (2013).
26. X. Li, S. Zhao, S. Pan, Z. Zhu, K. Qu, and T. Lin, "Generation of a frequency-quadrupled phase-coded signal using optical carrier phase shifting and balanced detection," *Appl. Opt.* **56**(4), 1151–1156 (2017).
27. W. Li, F. Kong, and J. Yao, "Arbitrary Microwave Waveform Generation Based on a Tunable Optoelectronic Oscillator," *IEEE Trans. Microw. Theory Tech.* **31**(23), 3780–3786 (2013).
28. S. Diddams, "The evolving optical frequency comb," *J. Opt. Soc. Am. B* **27**(11), B51–B62 (2010).
29. T. Sakamoto, "Optical Comb and Pulse Generation from CW Lightwave," in *International Topical Meeting on Microwave Photonics jointly held with the Asia-Pacific Microwave Photonics Conference*, Singapore, pp. 81–84, 2011.
30. Y. Chen, S. Liu, and S. Pan, "An optically tunable frequency-multiplying optoelectronic oscillator through equivalent phase modulation," in *2017 International Topical Meeting on Microwave Photonics*, Beijing, China, WEP. 23, 2017.
31. W. Li, M. Li, and J. Yao, "A narrow-passband and frequency-tunable micro-wave photonic filter based on phase-modulation to intensity-modulation conversion using a phase-shifted fiber Bragg grating," *IEEE Trans. Microw. Theory Tech.* **60**(5), 1287–1296 (2012).

1. Introduction

Microwave photonics, an interdisciplinary area which combines the worlds of radiofrequency (RF) engineering and optoelectronics, has been a topic of interest over the past few decades. The reason why microwave photonics is proposed is that some functions in traditional microwave systems are very complex or even impossible to be implemented directly in the electrical domain [1–3], whereas those are easy to be realized in the optical domain with the features of low loss, large bandwidth, large tunability and immunity to electromagnetic interference offered by modern photonics. In recent years, there has been an increasing effort both from the research community and the commercial sector in developing new microwave photonic techniques for various applications, such as optical and wireless communications, sensor networks, radar, imaging, software-defined radio, warfare systems and modern instrumentation [4,5]. Photonic generation of high-frequency microwave signals, phase-coded microwave signals and optical frequency combs is a hot topic covered by microwave photonics, which has attracted great interests in the past few years. Many research works in these topics were conducted.

In theory, a microwave signal can be generated by beating two optical wavelengths with correlated phases in a photodetector (PD), where the generated signal has a frequency equals to the frequency spacing of the two wavelengths. Many different approaches have been

proposed to generate the two wavelengths with correlated phases, such as optical phase-locked loop [6], optical injection locking [7], optical injection phase-locked loop [8], and optical nonlinear effect [9]. The two phase-correlated optical wavelengths for microwave signal generation can also be generated based on external modulation [10,11], which is a promising technique because of its simple structure and great flexibility. In addition, frequency multiplication can be easily implemented based on external modulation, leading to an effective solution to generate microwave signals with even higher frequency [12–15]. The phase noise of the generated signal using external modulation is mainly determined by the reference signal with a degradation of $20\log_{10}(N)$, where N is the frequency multiplication factor.

A low phase noise microwave signal can be generated using an optoelectronic oscillator (OEO), commonly consisting of a pump laser and a feedback circuit including a modulator, an optical fiber delay line, a PD, an amplifier and a filter [16]. Since the loss of optical fiber (0.2 dB/km) is very small, an OEO can employ a long optical fiber to obtain a loop with an ultra-high Q factor. A microwave signal with low phase noise can thus be generated when the OEO starts to oscillate. To further increase the frequency of the generated signal, frequency-multiplying OEOs were proposed. Frequency-doubled or quadrupled microwave signal is generated using an OEO operating at a low frequency in [17,18]. The major limitation in [17,18] is that the frequency multiplication factor is limited to two or four, and the system with a multiplication factor of four always needs an optical notch filter to filter out the optical carrier, so the ability of the system to generate low frequency signal is limited and the stability of the system is also decreased. To solve these problems, we propose a frequency-multiplying OEO with a tunable frequency multiplication factor without using optical filtering in [19], where frequency-quadrupled, sextupled or octupled microwave signal is generated with an OEO for the first time. The major disadvantage of the technique in [19] is that the frequency selection of the OEO is realized by an electrical band-pass filter (EBPF), which makes the frequency of the oscillation signal hard to be adjusted in a large frequency range.

On the other hand, the phase-coded microwave signal is the commonly used pulse compression signal in modern radar system to increase the range resolution and improve the signal-to-noise ratio (SNR) [20]. Phase-coded microwave signals can be generated in the optical domain to achieve high frequency tunability and large time-bandwidth product (TBWP) [21] through methods such as optical pulse shaping using free-space optics [22] or pure fiber optics [23], and optical external modulation [24–26]. To further simplify the structure and improve the performance of the phase-coded microwave signal generation scheme, OEOs are incorporated to generate phase-coded microwave signals, which features low phase noise and source-free operation [27].

Furthermore, optical frequency combs for multi-carriers and multi-tone generation using microwave photonics have also attracted increasing research attentions recently for applications in high-speed optical communication, arbitrary waveform generation and optical frequency reference [28]. External modulation is also suitable for optical frequency comb generation [29].

As discussed above, high-frequency microwave signals, phase-coded microwave signals and optical frequency combs are all able to be generated using external modulation with a RF reference, whereas OEOs provide an effective solution for low phase noise RF signal generation, which is a promising technique to offer reference signals with high performance. In [30], an OEO with a large frequency-tunable range based on equivalent phase modulation and phase modulation to intensity modulation conversion is proposed for frequency-quadrupled microwave signal generation using a dual-polarization quadrature phase shift-keying (DP-QPSK) modulator functioning in conjunction with a phase-shifted fiber Bragg grating (PS-FBG).

To further improve the scope of the application of the technique in [30], in this paper, the functionality of the OEO based system is explored from frequency quadrupling to frequency doubling, and from high-frequency microwave signal generation to phase-coded microwave signal generation and optical frequency comb generation. The key component of the proposed scheme is a DP-QPSK modulator. The upper dual-parallel Mach-Zehnder modulator (DP-MZM) integrated in the DP-QPSK modulator is properly biased to serve as an equivalent phase modulator (e-PM), which functions in conjunction with a PS-FBG in the OEO loop as a high-Q microwave photonic band-pass filter (MWP-BPF), whereas the lower DP-MZM in the DP-QPSK modulator injected by the oscillation signal functions as a frequency multiplier, a microwave phase-coded signal generator or an optical frequency comb generator, respectively, with different settings. To the best of our knowledge, it is the first OEO to realize frequency-quadrupled microwave signal generation with both large frequency tunability and no optical notch filter. A theoretical analysis is performed, which is verified by an experiment. A fundamental oscillation signal with a frequency from about 7.5 GHz to 12.5 GHz is generated in the OEO loop, which is used as the reference signals for frequency-doubled and quadrupled microwave signal generation up to 40 GHz, for fundamental and frequency-doubled binary phase-coded microwave signal generation up to 17 GHz, and for five-line optical frequency comb generation with a frequency spacing to 12.5 GHz. The frequency-tunable range of the system in this experiment is limited by the bandwidth of the PD and the electrical amplifier (EA) used in the OEO loop. Theoretically, the frequency-tunable range can be greatly increased by using PD and EA with a larger operating bandwidth.

2. Principle of operation

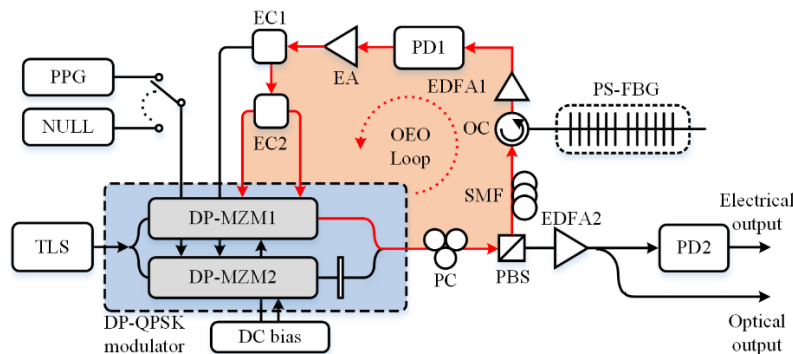


Fig. 1. Schematic diagram of the proposed OEO based multi-format signal generation approach. TLS, tunable laser source; DP-MZM, dual-parallel Mach-Zehnder modulator; PC, polarization controller; PBS, polarization beam splitter; EDFA, erbium-doped fiber amplifier; SMF, single-mode fiber; OC, optical circulator; PD, photodetector; PS-FBG, phase-shifted fiber Bragg grating; EA, electrical amplifier; EC, electrical coupler; PPG, pulse pattern generator.

The schematic diagram of the proposed OEO based multi-format signal generation approach is shown in Fig. 1. A continuous-wave (CW) light wave from a tunable laser source (TLS) is injected into a DP-QPSK modulator. The light wave is coupled to the two DP-MZMs integrated in the DP-QPSK modulator, where the polarization state of the optical signal at the output of DP-MZM2 is rotated by 90 degrees through a polarization rotator. The polarization rotated optical signal from DP-MZM2 is then combined with the orthogonally polarized optical signal from DP-MZM1. The modulated optical signal from the DP-QPSK modulator is sent to a polarization beam splitter (PBS) via a polarization controller (PC). The two principal axes of the PBS are aligned with those of the DP-QPSK modulator by tuning the PC. The PBS has two optical outputs. One output of the PBS is reflected by a PS-FBG via a

length of single-mode fiber (SMF) and an optical circulator (OC), and then amplified by an erbium-doped fiber amplifier (EDFA1) before being detected in PD1. The electrical signal generated from PD1 is amplified by an EA and then split into two paths by an electrical coupler (EC1): the electrical signal of one path is split by EC2 and applied to DP-MZM1 in the DP-QPSK modulator to close the OEO loop, which is shown in red line in Fig. 1; the electrical signal in the other path is applied to one RF port of DP-MZM2, and the other RF port of DP-MZM2 is connected to an pulse pattern generator (PPG) when phase-coded microwave signal is desired, or with no input when pure microwave signals or optical frequency combs are desired. The other output of the PBS is amplified by EDFA2 and then detected in PD2. With different settings, optical frequency combs can be generated at the output of EDFA2, and high-frequency microwave signals or phase-coded microwave signals can be generated at the output of PD2.

2.1 OEO loop

The main difference between the OEO shown in Fig. 1 and the classic OEO proposed in [16] is that the OEO in this paper does not employ an EBPF, which is the most important component in [16] to select the oscillation frequency among the possible oscillation modes in the OEO. The frequency selection in Fig. 1 is achieved using a MWP-BPF in the OEO loop. The DPMZM1 integrated in the DP-QPSK modulator is properly biased to serve as an e-PM, where the two sub-MZMs are biased at the minimum transmission point and the maximum transmission point, respectively, and the main-MZM is biased at the quadrature transmission point to introduce a 90-degree phase shift. The two electrical signals with equal amplitudes and phases from EC2 are applied to DP-MZM1, which are given by $V_1 \cos(\omega_s t)$, where V_1 is the amplitude and ω_s is the angular frequency of the microwave signal. The output of DP-MZM1 can be expressed as

$$\begin{aligned}
 E_1(t) &= E_1 \cos\left(\frac{\pi V_1 \cos(\omega_s t)}{2V_\pi}\right) \exp(j\omega_c t) \\
 &+ E_1 \cos\left(\frac{\pi(V_1 \cos(\omega_s t) - V_\pi)}{2V_\pi}\right) \exp\left(j\omega_c t + j\frac{\pi}{2}\right) \\
 &= E_1 \left[\cos(\gamma \cos(\omega_s t)) + j \sin(\gamma \cos(\omega_s t)) \right] \exp(j\omega_c t) \\
 &= E_1 \exp(j\omega_c t + j\gamma \cos(\omega_s t)),
 \end{aligned} \tag{1}$$

where E_1 is the amplitude and ω_c is the angular frequency of the optical signal, V_π is the half-wave voltage of the DP-QPSK modulator, $\gamma = \pi V_1 / 2V_\pi$. It is observed from Eq. (1) that the electrical signal applied to DP-MZM1 is phase modulated onto the optical carrier. The expression in Eq. (1) is the same as that at the output of a phase modulator (PM), so equivalent phase modulation is achieved in DP-MZM1.

The optical signal at the output of DP-MZM1 is routed to a PS-FBG via a PBS, a length of SMF and an OC. The PS-FBG has an ultra-narrow notch on its reflection spectrum. When an optical phase-modulated signal with its carrier located on the flat reflection spectrum is injected into the PS-FBG, the ultra-narrow notch filters out some part of the phase-modulated signal in frequency domain and converts the phase-modulated signal to an intensity-modulated signal, which can thus be detected by a square-law PD. By beating the reflected optical signal from the PS-FBG at PD1, a high-Q tunable MWP-BPF is obtained. The central frequency of the filter is determined by the frequency spacing between the optical carrier and the narrow notch on the reflection spectrum of the PS-FBG, which can be tuned by adjusting the wavelength of the TLS. The electrical signal generated from PD1 is amplified by an EA

and then applied to DP-MZM1 via EC1 and EC2 to close the loop and form an OEO. When the net gain of the OEO loop is greater than 1, the OEO starts to oscillate from noise transient, which is then built up and sustained with feedback at the level of the oscillator output signal. When the OEO oscillates stably, a fundamental signal is generated in the OEO loop with its frequency determined by the central frequency of the high-Q MWP-BPF.

2.2 Frequency-multiplying microwave signal generation

To generate frequency-multiplying microwave signal, the oscillation frequency in the OEO loop is power divided by a 1:1 EC. One half of the oscillation signal is re-applied to DP-MZM1 to maintain the oscillation in the OEO, and the other half of the oscillation signal is applied to one of the RF ports of DP-MZM2, which functions as a frequency multiplier with a tunable frequency multiplication factor. The other RF port of DP-MZM2 is with no input.

For frequency-doubled microwave signal generation, the sub-MZM in DP-MZM2 with oscillation signal applied is biased at the minimum transmission point, whereas the main-MZM is biased to introduce a 180-degree phase shift. Under these conditions, the optical signal at the output of DP-MZM2 can be expressed as

$$\begin{aligned} E_{doubled}(t) &= E_2 \cos\left(\frac{\pi V_b}{2V_\pi}\right) \exp(j\omega_c t + j\pi) + E_2 \cos\left(\frac{\pi(V_2 \cos(\omega_s t) - V_\pi)}{2V_\pi}\right) \exp(j\omega_c t) \\ &= \left[\sin(\delta \cos(\omega_s t)) - \cos(\xi) \right] E_2 \exp(j\omega_c t) \\ &= \left[-2 \sum_{n=1}^{\infty} (-1)^n J_{2n-1}(\delta) \cos((2n-1)\omega_s t) - \cos(\xi) \right] E_2 \exp(j\omega_c t), \end{aligned} \quad (2)$$

where J_n is the n th-order Bessel function of the first kind, E_2 is the amplitude of the optical signal, V_b is the bias voltage of the sub-MZM with no RF input, V_2 is the amplitude of the microwave signal, $\xi = \pi V_b / 2V_\pi$, $\delta = \pi V_2 / 2V_\pi$. As shown in Eq. (2), the optical signal at the output of DP-MZM2 consists of odd-order optical sidebands from one sub-MZM and an optical carrier from the other sub-MZM. To generate a frequency-doubled microwave signal, the optical carrier is suppressed by setting $\cos(\xi) = 0$, i.e. $\xi = 2.405$, $V_b = 1.53V_\pi$. Under small signal modulation condition ($\delta \ll 1$), Eq. (2) can be simplified as

$$E_{doubled}(t) \approx 2E_2 J_1(\delta) \cos(\omega_s t) \exp(j\omega_c t), \quad (3)$$

where only two first-order optical sidebands are generated. Applying the optical signal to a square-law PD (PD2), the photocurrent can be expressed as

$$\begin{aligned} i_{doubled}(t) &= R |E_{doubled}(t)|^2 = RE_{doubled}(t) E_{doubled}^*(t) \\ &= 4RE_2^2 J_1^2(\delta) \cos^2(\omega_s t) \\ &= 2RE_2^2 J_1^2(\delta) + 2RE_2^2 J_1^2(\delta) \cos(2\omega_s t), \end{aligned} \quad (4)$$

where R is the responsivity of PD2. At the output of PD2, a microwave signal with a carrier frequency at $2\omega_s$ is generated besides a direct current.

For frequency-quadrupled microwave signal generation, the sub-MZM in DP-MZM2 with oscillation signal applied is biased at the maximum transmission point, whereas the main-MZM is biased to introduce a 180-degree phase shift. Under these conditions, the optical signal at the output of DP-MZM2 can be expressed as

$$\begin{aligned}
 E_{quadrupled}(t) &= E_2 \cos\left(\frac{\pi V_b}{2V_\pi}\right) \exp(j\omega_c t + j\pi) + E_2 \cos\left(\frac{\pi V_2 \cos(\omega_s t)}{2V_\pi}\right) \exp(j\omega_c t) \\
 &= \left[\cos(\delta \cos(\omega_s t)) - \cos(\xi) \right] E_2 \exp(j\omega_c t) \\
 &= \left[J_0(\delta) + 2 \sum_{n=1}^{\infty} (-1)^n J_{2n}(\delta) \cos(2n\omega_s t) - \cos(\xi) \right] E_2 \exp(j\omega_c t).
 \end{aligned} \tag{5}$$

As shown in Eq. (5), the optical signal at the output of DP-MZM2 consists of even-order optical sidebands, an optical carrier from one sub-MZM and another optical carrier from the other sub-MZM. By setting $\cos(\xi) = J_0(\delta)$, the two optical carriers from two sub-MZMs cancel each other. Under small signal modulation condition ($\delta \ll 1$), Eq. (5) can be simplified as

$$E_{quadrupled}(t) \approx -2E_2 J_2(\delta) \cos(2\omega_s t) \exp(j\omega_c t). \tag{6}$$

As shown in Eq. (6), only two second-order optical sidebands are generated. Beating the optical signal at PD2, the photocurrent can be expressed as

$$\begin{aligned}
 i_{quadrupled}(t) &= R |E_{quadrupled}(t)|^2 = RE_{quadrupled}(t) E_{quadrupled}^*(t) \\
 &= 4RE_2^2 J_2^2(\delta) \cos^2(2\omega_s t) \\
 &= 2RE_2^2 J_2^2(\delta) + 2RE_2^2 J_2^2(\delta) \cos(4\omega_s t),
 \end{aligned} \tag{7}$$

At the output of PD2, a microwave signal with a carrier frequency at $4\omega_s$ is generated besides a direct current.

The principle of the generation process of frequency-doubled and quadrupled microwave signals discussed above is shown in Fig. 2.

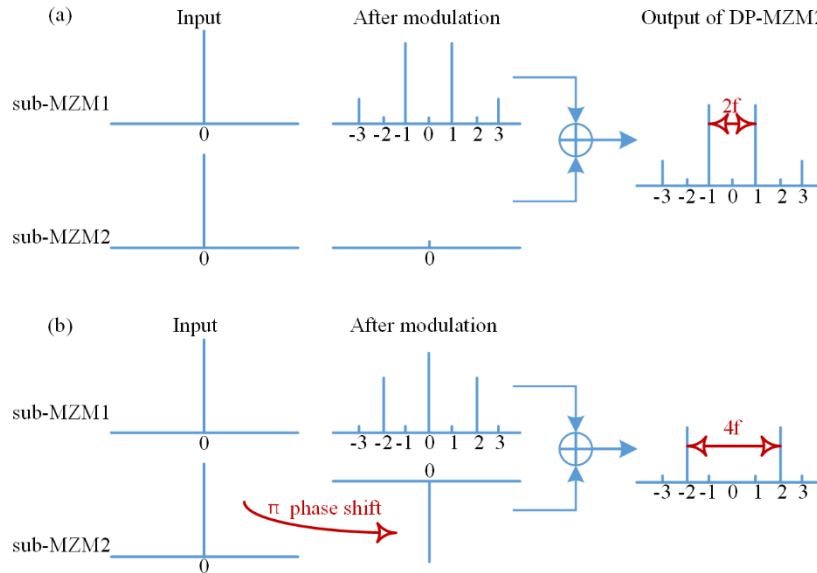


Fig. 2. Principle of the generation process of (a) frequency-doubled and (b) quadrupled microwave signals.

2.3 Phase-coded microwave signal generation

For phase-coded microwave signal generation, the oscillation frequency in the OEO loop is power divided by a 1:1 EC. One half of the oscillation signal is re-applied to DP-MZM1 to maintain the oscillation of the OEO, and the other half of the oscillation signal is applied to one of the RF ports of DP-MZM2. The other RF port of DP-MZM2 is injected by an electrical coding signal from a PPG. The DP-MZM2 integrated in the DP-QPSK modulator functions as a phase-coded signal generator.

Assuming the coding signal is $V_s s(t)$ and the oscillation signal applied to DP-MZM2 is $V_2 \cos(\omega_s t)$, the optical signal at the output of DP-MZM2 is expressed as

$$\begin{aligned} E_{coding}(t) &= E_2 \cos\left(\frac{\pi(V_s s(t) - V_{DC1})}{2V_\pi}\right) \exp(j\omega_c t + j\varphi) \\ &+ E_2 \cos\left(\frac{\pi(V_2 \cos(\omega_s t) - V_{DC2})}{2V_\pi}\right) \exp(j\omega_c t) \\ &= \left[\cos(\gamma s(t) - \theta_1) \exp(j\varphi) + \cos(\kappa \cos(\omega_s t) - \theta_2) \right] E_2 \exp(j\omega_c t), \end{aligned} \quad (8)$$

where V_s is the amplitude of the coding signal, V_{DC1} and V_{DC2} are the bias voltages of the two sub-MZMs, respectively, φ is the phase shift introduced by the main-MZM, $\theta_1 = \pi V_{DC1} / 2V_\pi$, $\theta_2 = \pi V_{DC2} / 2V_\pi$, $\gamma = \pi V_s / 2V_\pi$, $\kappa = \pi V_2 / 2V_\pi$. Beating the optical signal at PD2, the photocurrent from PD2 can be expressed as

$$\begin{aligned} i_{coding}(t) &= R |E_{coding}(t)|^2 = RE_{coding}(t) E_{coding}^*(t) \\ &= RE_2^2 \cos^2(\gamma s(t) - \theta_1) + RE_2^2 \cos^2(\kappa \cos(\omega_s t) - \theta_2) \\ &+ 2RE_2^2 \cos \varphi \cos(\gamma s(t) - \theta_1) \cos(\kappa \cos(\omega_s t) - \theta_2) \\ &= RE_2^2 \cos^2(\gamma s(t) - \theta_1) + \frac{1}{2} RE_2^2 + \frac{1}{2} RE_2^2 \cos(2\kappa \cos(\omega_s t) - 2\theta_2) \\ &+ 2RE_2^2 \cos \varphi \cos(\gamma s(t) - \theta_1) \cos(\kappa \cos(\omega_s t) - \theta_2). \end{aligned} \quad (9)$$

When $\theta_1 = \theta_2 = \pi/2$ establishes, and the system operate under the small signal modulation condition ($\kappa \ll 1$), Eq. (9) can be simplified as

$$\begin{aligned} i_{fundamental}(t) &= \frac{1}{2} RE_2^2 + RE_2^2 \sin^2(\gamma s(t)) - \frac{1}{2} RE_2^2 \cos(2\kappa \cos(\omega_s t)) \\ &+ 2RE_2^2 \cos \varphi \sin(\gamma s(t)) \sin(\kappa \cos(\omega_s t)) \\ &\approx RE_2^2 \left[\frac{1}{2} - \frac{1}{2} J_0(2\kappa) \right] + RE_2^2 \sin^2(\gamma s(t)) + RE_2^2 J_2(2\kappa) \cos(2\omega_s t) \\ &+ 2RE_2^2 \kappa \cos \varphi \sin(\gamma s(t)) \cos(\omega_s t). \end{aligned} \quad (10)$$

As shown in Eq. (10), the first term in Eq. (10) is a direct current, the second term is a baseband modulation product, the third term is pure second-order harmonic at $2\omega_s$, and the fourth term is a coding signal at ω_s . When $s(t)$ is a bipolar signal ($+1, -1$) and $\gamma \neq n\pi$ (n is an integer) establish, the microwave signal at ω_s has two phases with π phase difference with different values of $s(t)$. To maximize the amplitude of the generated phase-coded

signal, we choose $\gamma = 0.5\pi$ and $\varphi = 0$, so the phase-coded microwave signal in Eq. (10) can be expressed as

$$i_{\text{fundamental}}(t) = 2RE_2^2 \kappa \sin(0.5\pi s(t)) \cos(\omega_s t) = \begin{cases} 2RE_2^2 \kappa \cos(\omega_s t) & s(t) = 1 \\ 2RE_2^2 \kappa \cos(\omega_s t + \pi) & s(t) = -1. \end{cases} \quad (11)$$

A binary phase-coded microwave signal at the fundamental oscillation frequency is generated.

To generate frequency-doubled binary phase-coded microwave signal, we set $\theta_1 = \pi/2$ and $\theta_2 = 0$ in Eq. (9), so it can be simplified as

$$\begin{aligned} i_{\text{doubled}}(t) &= \frac{1}{2} RE_2^2 + RE_2^2 \sin^2(\gamma s(t)) + \frac{1}{2} RE_2^2 \cos(2\kappa \cos(\omega_s t)) \\ &\quad + 2RE_2^2 \cos(\varphi) \sin(\gamma s(t)) \cos(\kappa \cos(\omega_s t)) \\ &\approx RE_2^2 \left[\frac{1}{2} + \frac{1}{2} J_0(2\kappa) \right] + RE_2^2 \sin^2(\gamma s(t)) + 2RE_2^2 J_0(\kappa) \cos(\varphi) \sin(\gamma s(t)) \\ &\quad - RE_2^2 \left[J_2(2\kappa) + 4J_2(\kappa) \cos(\varphi) \sin(\gamma s(t)) \right] \cos(2\omega_s t). \end{aligned} \quad (12)$$

As shown in Eq. (12), the first term in Eq. (10) is a direct current, the second and third terms are baseband modulation products, the fourth term is a coding signal at $2\omega_s$. When $s(t)$ is a bipolar signal ($+1, -1$), $J_2(2\kappa) = 0$ ($\kappa = 2.57$) and $\gamma \neq n\pi$ (n is an integer) establish, the microwave signal at $2\omega_s$ has two phases with π phase difference with different values of $s(t)$. To maximize the amplitude of the generated phase-coded signal, we also choose $\gamma = 0.5\pi$ and $\varphi = 0$, so the phase-coded microwave signal in Eq. (12) can be expressed as

$$i_{\text{doubled}}(t) = -4RE_2^2 J_2(\kappa) \sin(0.5\pi s(t)) \cos(2\omega_s t) = \begin{cases} 4RE_2^2 J_2(\kappa) \cos(2\omega_s t + \pi) & s(t) = 1 \\ 4RE_2^2 J_2(\kappa) \cos(2\omega_s t) & s(t) = -1. \end{cases} \quad (13)$$

A frequency-doubled phase-coded microwave signal is generated.

For the novel method proposed in this paper to generate a frequency-doubled binary phase-coded microwave signal via a DP-MZM in the DP-QPSK modulator, high modulation index is required to suppress the pure microwave signal at the doubled frequency. For a DP-QPSK modulator with a half-wave voltage of 3.5 V, the modulation voltage applied to the DP-MZM is about 2.86 V, which is within the maximum allowable applied voltage range of the DP-QPSK modulator.

2.4 Optical frequency comb generation

For optical frequency comb generation, the oscillation frequency in the OEO loop is power divided by a 1:1 EC. One half of the oscillation signal is re-applied to DP-MZM1 to maintain the oscillation of the OEO, and the other half of the oscillation signal is applied to one of the RF ports of DP-MZM2, which functions as an optical frequency comb generator with a tunable frequency. The other RF port of DP-MZM2 is with no input. The bias voltages of DP-MZM2 are V_b and V_{Bias} . The optical signal at the output of DP-MZM2 can be expressed as

$$\begin{aligned}
E_{comb}(t) &= E_2 \cos\left(\frac{\pi V_b}{2V_\pi}\right) \exp(j\omega_c t) + E_2 \cos\left(\frac{\pi(V_2 \cos(\omega_s t) - V_{bias})}{2V_\pi}\right) \exp(j\omega_c t) \\
&= E_2 \left\{ \cos(\xi) + \cos\Theta \cos(\delta \cos(\omega_s t)) + \sin\Theta \sin(\delta \cos(\omega_s t)) \right\} \exp(j\omega_c t) \quad (14) \\
&\approx E_2 \left\{ \cos(\xi) + \cos\Theta J_0(\delta) + [2 \sin\Theta J_1(\delta) \cos(\omega_s t) - 2 \cos\Theta J_2(\delta) \cos(2\omega_s t) \right. \\
&\quad \left. - 2 \sin\Theta J_3(\delta) \cos(3\omega_s t) + 2 \cos\Theta J_4(\delta) \cos(4\omega_s t) \right\} \exp(j\omega_c t),
\end{aligned}$$

where $\xi = \pi V_b / 2V_\pi$, $\delta = \pi V_2 / 2V_\pi$, $\Theta = \pi V_{bias} / 2V_\pi$. For five-line optical frequency comb generation, the optical carrier, the first-order optical sidebands and the second-order optical sidebands are equal in power when

$$\cos(\xi) + \cos\Theta J_0(\delta) = \sin\Theta J_1(\delta) = \cos\Theta J_2(\delta). \quad (15)$$

Figure 3 shows the characteristics of the Bessel function of the first kind. It is observed from Fig. 3 that the power ratio of the first-order sideband to the third-order sideband, i.e. $20 \log_{10}(J_1(\delta) / J_3(\delta))$, is decreasing when δ is increasing from 0 to 3.054, which means a smaller modulation index in this range will lead to a better suppression of the third-order sideband. To better suppress sidebands higher than the second order, a small δ is required for the generation of the five-line optical frequency comb. Other parameters, such as ξ and Θ , can be further obtained by solving Eq. (15).

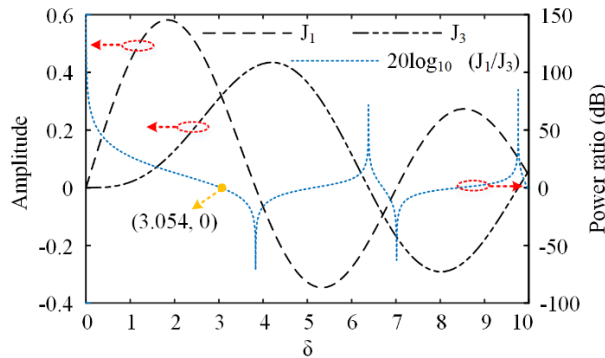


Fig. 3. Characteristics of the Bessel function of the first kind.

There is a special δ in Fig. 3, where the power of the first-order sidebands and the third-order sidebands is identical. If the system is operating at this condition ($\delta=3.054$), a seven-line optical frequency comb can be generated. The power ratio of the desired frequency comb to the undesired fourth-order sideband can be calculated using Eq. (14), which is 10.86 dB. However, for the seven-line frequency comb generation, the modulation index relatively high (3.054) and fixed, thus leading to a small mode suppression ratio. In comparison, for five-line optical frequency generation, the mode suppression ratio can be adjusted by using different modulation index.

3. Experimental results and discussion

An experiment based on the setup shown in Fig. 1 is performed. A CW light wave with 10 dBm power generated from an TLS (Teraxion PS-TNL) is injected into a DP-QPSK modulator (Fujitsu FTM7977). The DP-QPSK modulator has a 3-dB modulation bandwidth of 23 GHz and an insertion loss of 13 dB. The optical signal at the output of the DP-QPSK modulator is sent to a PBS via a PC, with two principal axes of the PBS aligned with those of

the DP-QPSK modulator. One output of the PBS is reflected in a PS-FBG (Teraxion) with an ultra-narrow notch of about 40 MHz (3 dB) via an SMF and an OC, and then amplified by EDFA1 (Amonics) before being detected in PD1 (Conquer) with a 3-dB bandwidth of 11.5 GHz. The output of PD1 is amplified by EA (a low phase noise amplifier with a bandwidth from 8 GHz to 18 GHz cascaded with a power amplifier with a bandwidth from 6 GHz to 18 GHz) and then sent to three of the four RF ports of the DP-QPSK modulator via two ECs. The other RF port of the DP-QPSK modulator is driven by a PPG (Anritsu MP1763C) for phase-coded microwave signal generation or with no inputs for pure microwave signal generation and optical frequency comb generation. The other output of the PBS is amplified by EDFA2 (Amonics). When pure microwave signal generation and optical frequency comb are desired, the optical signal after amplification is detected by PD2 (u2t) with a 3-dB bandwidth of 40 GHz.

3.1 Oscillation signal generation

The fundamental oscillation frequency of the system is determined by the frequency spacing between the central optical wavelength and the ultra-narrow notch on the reflection spectrum of the PS-FBG, which is also the central frequency of the MWP-BPF. The notch of the PS-FBG is fabricated at about 1549.99 nm. The wavelength of the TLS is located at about 7.5 GHz away from the notch, and then tuned at a step of about 1 GHz. The frequency response of the MWP-BPF is measured using a vector network analyzer (R&S ZVA-67) by open the OEO loop at the output of PD1.

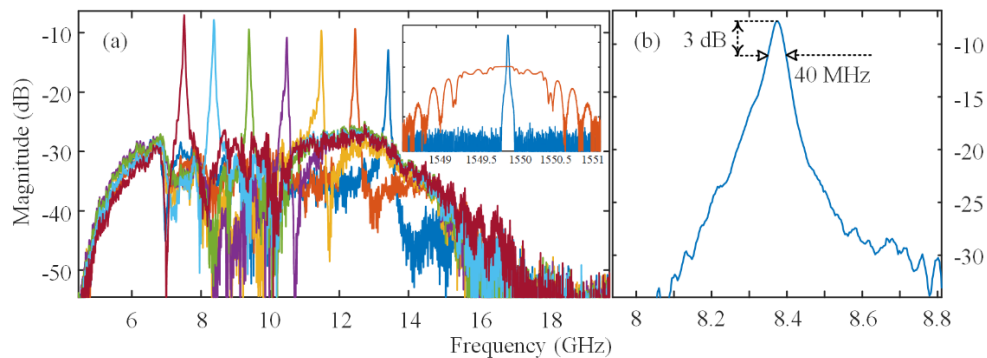


Fig. 4. (a) Measured frequency response of the tunable MWP-BPF. (b) Zoom-in view of the frequency response when the central frequency is at 8.376 GHz. The inset in (a) shows the reflection spectrum of the PS-FBG and an optical carrier located on it.

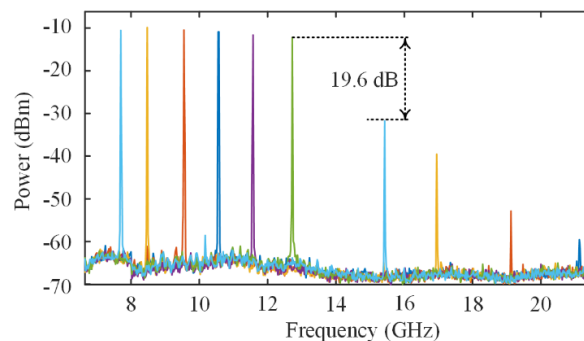


Fig. 5. Electrical spectra of the generated oscillation signals in the OEO loop with the frequency tuned from 7.5 GHz to 12.7 GHz.

Figure 4(a) shows the frequency response of the tunable MWP-BPF. Since the bandwidth of PD1 and EA are limited, the central frequency of the filter is only tuned between about 7.5 GHz to 13.5 GHz. The response of the filter is significantly decreased when the central frequency is higher than 12.5 GHz, which is limited by the bandwidth of PD1. Figure 4(b) shows a zoom-in view of the measured response of the MWP-BPF when the central frequency is 8.376 GHz. The 3-dB bandwidth of the filter is 40 MHz, which is equal to the 3-dB bandwidth of the ultra-narrow notch of the PS-FBG. The inset in Fig. 4(a) shows the reflection spectrum of the PS-FBG measured by the optical spectrum analyzer (OSA, Yokogawa AQ6370C). The ultra-narrow notch on the reflection spectrum is not observed due to the limited resolution of the OSA.

Figure 5 shows the spectra of the oscillation signals in the OEO loop. The frequency is tuned by adjusting the wavelength of the TLS. Second harmonics at doubled-frequencies are also observed in the spectra, which is generated by the nonlinearity of the optical modulation. The power ratios of the oscillation signals to the harmonics due to the nonlinear modulation are about 20 dB. Since the EA used in the experiment has an operation frequency of less than 18 GHz, the second harmonics are better suppressed at the frequency above 18 GHz.

3.2 Frequency-multiplying microwave signal generation

The oscillation signals shown in Fig. 5 are used for frequency-multiplying microwave signal generation. Taking the bandwidth of PD2 and EA into consideration, we choose the oscillation signals at 8.50 GHz, 9.55 GHz, 10.58 GHz, 11.58 GHz, 12.66 GHz for frequency-doubled microwave signal generation, and at 8.50 GHz, 9.55 GHz, 10.58 GHz for frequency-quadrupled microwave signal generation.

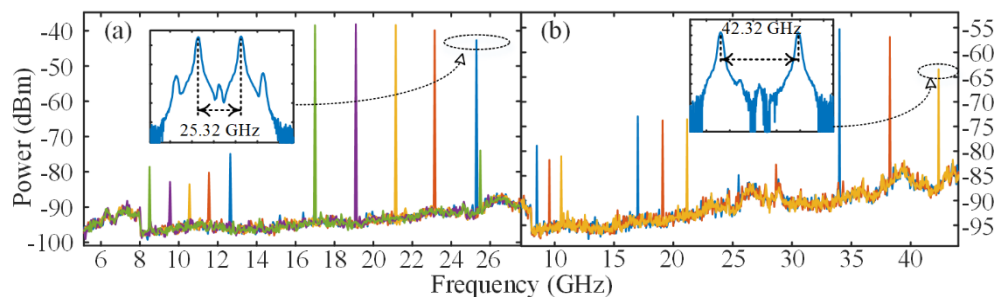


Fig. 6. Electrical spectra of the generated (a) frequency-doubled and (b) frequency-quadrupled microwave signals. The insets are the corresponding optical spectra at the input of EDFA2.

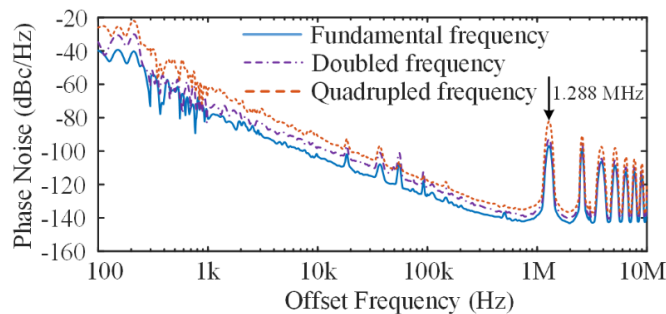


Fig. 7. Phase-noise performance for the fundamental (8.50 GHz), frequency-doubled (17.00 GHz) and frequency-quadrupled (34.00 GHz) microwave signals.

As shown in Fig. 6(a), frequency-doubled microwave signals at 17.00 GHz, 19.10 GHz, 21.16 GHz, 23.16 GHz and 25.32 GHz are generated. The fundamental frequency is more than 25 dB suppressed. The inset in Fig. 6(a) is the corresponding optical spectrum for 25.32

GHz microwave signal generation. Figure 6(b) demonstrates the spectra of the generated frequency-quadrupled microwave signals at 34.00 GHz, 38.20 GHz and 42.32 GHz. The power of the microwave signal at 42.32 GHz is much lower than the other two frequencies, which is caused by the lower frequency response at 42.32 GHz limited by the bandwidth of PD2 (40 GHz). The fundamental and doubled frequencies are also generated with suppression ratios of more than 17 dB. The suppression of harmonics for frequency-quadrupled microwave signal generation is not that good as in [19], which could be caused by the non-ideal polarization direction alignment between the DP-QPSK modulator and the PBS. The inset in Fig. 6(b) is the corresponding optical spectrum for 42.32 GHz microwave signal generation.

The phase-noise performance of the fundamental frequency at 8.50 GHz and the frequency-multiplying signals at 17.00 GHz and 34.00 GHz is also evaluated, which is measured by a phase noise analyzer (R&S FSWP-50), and shown in Fig. 7. As can be seen, a phase noise performance degradation is introduced in the process of frequency multiplying. In addition, some peaks at integral multiples of 1.288 MHz are observed, which are the eigenmodes in the OEO loop determined by the free spectral range of the loop.

The frequency of the fundamental signal in the OEO loop as well as the frequency of the frequency-multiplying microwave signal can be further increased by employing components with larger operation bandwidths. However, the operation bandwidths of the components in the OEO loop can be greatly reduced compared with the frequency band of the generated microwave signal through the frequency-multiplying OEO. For high frequency signal generation, only PD2 needs to have large bandwidth. The bandwidths of the components in the OEO loop only need to be 1/4 of PD2.

3.3 Phase-coded microwave signal generation

For the phase-coded microwave signal generation, we use the oscillation signal in the OEO loop as the reference applied to one RF port of DP-MZM2, and the coding signal generated from a PPG is applied to the other RF port of DP-MZM2. The frequency of the generated phase-coded microwave signal is tunable by tuning the frequency of the oscillation signal in the OEO loop. The generated phase-coded microwave signal is monitored by a digital sampling oscilloscope (DSO, Agilent DCA-J 86100C). The connection of the measurement system is shown in Fig. 8.

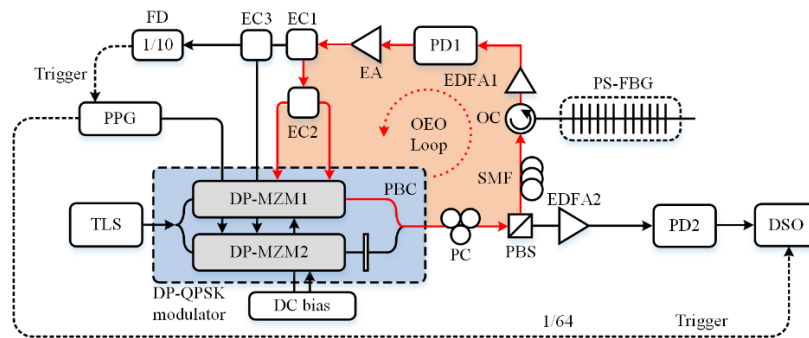


Fig. 8. Setup for phase-coded microwave signal measurement. FD, frequency divider.

The PPG is triggered by the oscillation signal from the OEO loop via a 1/10 frequency divider (FD). Therefore, the clock of the PPG as well as the data rate of the coding signal is 1/10 the frequency of the oscillation signal. The DSO is triggered by the PPG with 1/64 the clock of the PPG.

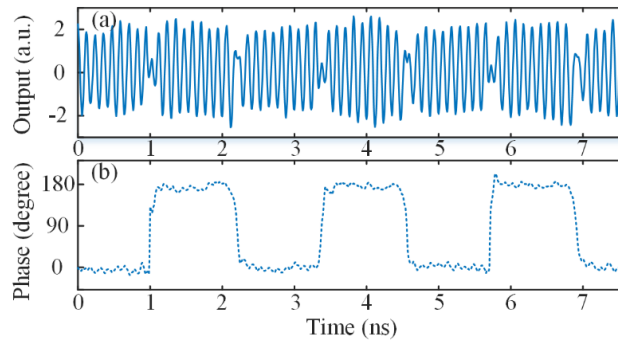


Fig. 9. (a) Generated 8.50 GHz phase-coded microwave signal, (b) recovered phase information from (a).

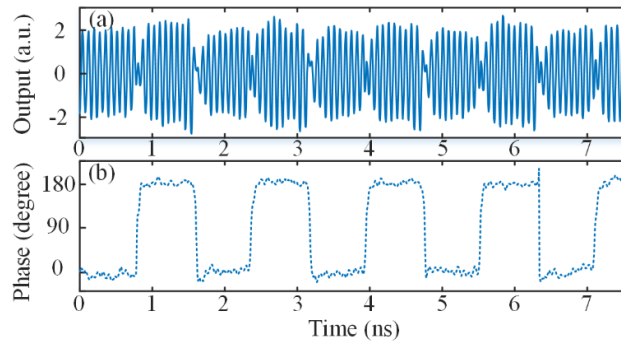


Fig. 10. (a) Generated 12.66 GHz phase-coded microwave signal, (b) recovered phase information from (a).

First, the coding signal from the PPG is a “0101” sequence. The oscillation signal in the OEO loop is 8.50 GHz, so the data rate of the coding signal is 850 Mbps. The generated phase-coded microwave signal and the recovered phase information using Hilbert transform are shown in Fig. 9. It is obvious that there is a phase jump in the microwave waveform, and a 180-degree phase shift is obtained from the phase information as predicted in the theoretical section. Then, the oscillation signal is tuned to 12.66 GHz to demonstrate the frequency tunability of the system, so the data rate of the coding signal from the PPG is 1.266 Gbps. It is also observed from Fig. 10 that a phase jump in the microwave waveform shown in Fig. 10(a), and a 180-degree phase shift is obtained in Fig. 10(b).

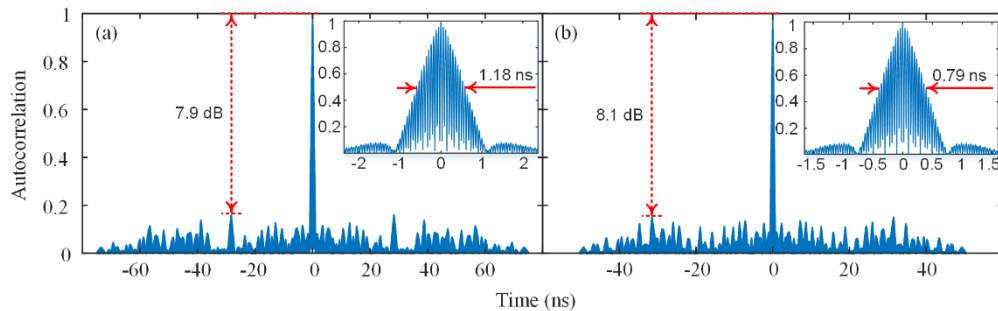


Fig. 11. Autocorrelation of the generated 64-bit phase-coded microwave signal with a carrier frequency at (a) 8.50 GHz, (b) 12.66 GHz. The insets are the zoom-in views of the autocorrelation peaks.

The pulse autocorrelation is very important to defined the performance because radar receiver operates the cross correlation between the microwave pulse and its echo to get a compressed pulse. The PPG has a 1/64 clock output, which is used to trigger the DSO. To simplify the experiment, we only use 64-bit pseud-random bit sequence (PRBS) to verify the pulse compression performance of the system to avoid adding another FD for bit sequence longer than 64 bits. The 64-bit PRBS used in this experiment is optimized by choosing one from about one hundred 64-bit PRBSs using Matlab, which has the best peak-to-sidelobe ratio (PSR) of about 8.52 dB among all the sequence. Figure 11 shows the autocorrelations of the generated phase-coded microwave signals. The zoom-in views shown in the insets exhibit a full width at half-maximum (FWHM) of 1.18 ns for the 8.50 GHz signal and 0.79 ns for the 12.66 GHz signal. The corresponding pulse compression ratios (PCR) are about 64 for both cases, which is consistent with the theoretical values. The PSRs are 7.9 dB for the 8.50 GHz signal and 8.1 dB for the 12.66 GHz signal.

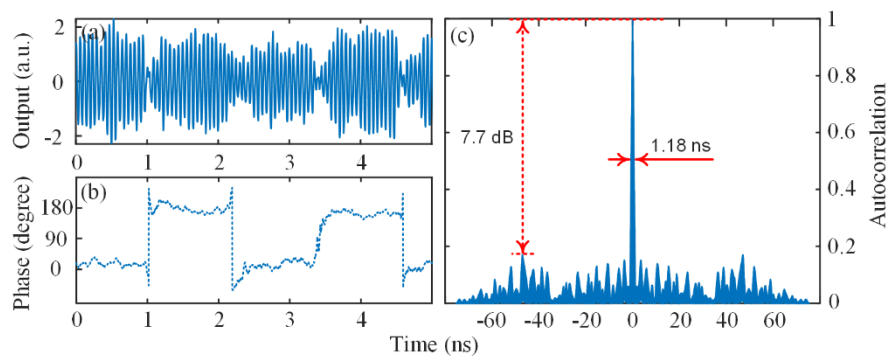


Fig. 12. (a) Generated 17.00 GHz phase-coded microwave signal, (b) recovered phase information from (a), (c) Autocorrelation of the generated 64-bit phase-coded microwave signal with a carrier frequency at 17.00 GHz.

The system is then tuned to generate a frequency-doubled phase-coded microwave signal to verify the functionality of frequency doubling of the system. The oscillation frequency is 8.50 GHz, and the data rate of the coding signal from the PPG is 850 Mbps. A 17.00-GHz phase-coded microwave signal is generated, which is shown in Fig. 12(a). The recovered phase information is shown in Fig. 12(b). Pulse compression performance is also evaluated, which is shown in Fig. 12(c), where a PSR of 7.7 dB and a PCR of about 64 are obtained.

3.4 Optical frequency comb generation

For the optical frequency comb generation, the oscillation signals are used as the reference. The frequency spacing of the optical frequency comb is determined by the oscillation frequency.

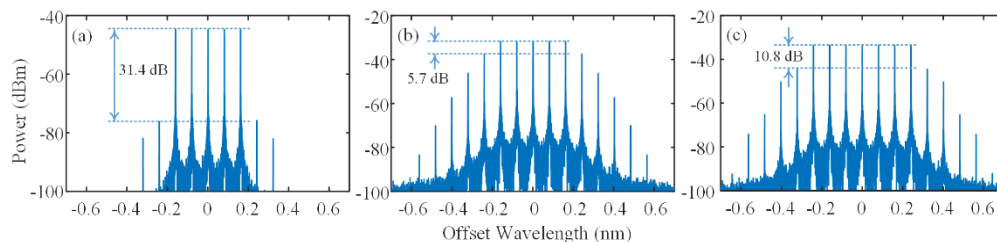


Fig. 13. Simulated five-line optical frequency comb with different working points. (a) δ equals to 0.7945, (b) δ equals to 2.6299. (c) Simulated seven-line optical frequency comb.

As discussed in Section 2.4, for the five-line frequency comb generation, a small δ is required to better suppress sidebands higher than the second order. We simulated two optical frequency combs with different δ to validate the theory, where $\sin \Theta$ equals to 0.2, Θ is 0.2014, δ is 0.7945, and ξ is 2.5520, or $\sin \Theta$ equals to 0.7071, Θ is 0.7854, δ is 2.6299, and ξ is 1.1535. The simulation results are shown in Fig. 13(a) and (b). The condition with a smaller δ has a mode suppression ratio of 31.4 dB, while that for the condition with a larger δ is only 5.7 dB. However, the power of the generated frequency comb is larger when δ is 2.6299. There is a tradeoff between the power and the mode suppression ratio of the generated five-line optical frequency comb. For the seven-line optical frequency comb generation, only a set of parameters can be used, i.e. $\Theta=0.9909$, $\delta=3.0542$, $\xi=1.1387$. The simulated seven-line optical frequency is shown in Fig. 13(c), where the mode suppression ratio is fixed to 10.8 dB.

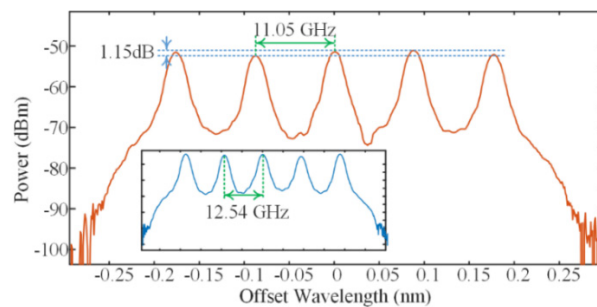


Fig. 14. Generated optical frequency comb with a frequency spacing of 11.05 GHz. The inset is the generated optical frequency comb with a frequency spacing of 12.54 GHz.

Since the modulation index required for the seven-line optical frequency comb is very large, and the mode suppression ratio is only 10.8 dB, we only verify the generation of five-line frequency comb. In the experiment, the oscillation frequency of the OEO is tuned to 11.05 GHz. We select a small δ around 0.7945, and the experimentally generated optical frequency comb is shown in Fig. 14. It is observed that the other modes in the optical spectra is deeply suppressed, and only five lines are generated. The flatness of the optical frequency comb is about 1.15 dB. The frequency spacing of the optical frequency comb can be tuned by tuning the oscillation frequency in the OEO. The inset in Fig. 14 shows the generated optical frequency comb when the oscillation frequency of the OEO is 12.54 GHz to demonstrate the frequency tunability of the system.

3.5 Discussion

Thanks to the simple and compact structure, the proposed multi-format signal generation system can be operated stably. The operation frequency range of the proposed system is mainly limited by bandwidth of the components in the OEO loop, especially the PS-FBG. With a PS-FBG with larger reflection bandwidth and components with corresponding bandwidths, the frequency-tunable range of the OEO can be enhanced to tens of GHz or hundreds of GHz [31]. However, the DP-QPSK modulator only has a 3-dB bandwidth of 23 GHz, which constrains the theoretical oscillation frequency to 23 GHz. In fact, we need large bandwidth only for single frequency modulation and oscillation in the OEO loop, so the flatness of the response of the DP-QPSK modulator is not particularly important. The 6-dB bandwidth of the DP-QPSK modulator is about 50 GHz. It means if we operate the DP-QPSK modulator in that frequency range, only 3-dB additional optical power loss is introduced, which can be compensated by optical or electrical amplification. Therefore, with enough bandwidth of the components in the OEO loop, the OEO can be operated up to 50 GHz, which means we can generate pure microwave signals up to 200 GHz, phase-coded

microwave signals up to 100 GHz, and optical frequency combs with frequency spacing up to 50 GHz, if PD2 has corresponding large bandwidth. For the coding signal used for phase-coded microwave signal generation, its data rate is limited to 31.4 Gbps because the DP-QPSK modulator has a modulation speed of up to 31.4 Gbaud.

Equivalent phase modulation in this paper is a novel method to realize phase modulation in a DP-MZM by properly choosing the bias points of the DP-MZM. It is an accurate phase modulation, which is completely the same as that being done by a PM. To obtain an accurately 100% phase modulation via a DP-MZM, bias point must be controlled precisely. In our experiment, the DC bias are supplied by DC power supply. In long term operation, the bias points of the modulator may drift from the desired points, which may influence the performance and stability of the system. However, if this technique is to be used in actual product, the bias accurate is not a problem because the bias control technique for DP-MZM is well researched and commercially available.

4. Conclusion

In conclusion, a multi-format signal generation approach using a frequency-tunable OEO is proposed and experimentally investigated. The key contribution of the work is that one DP-MZM in the DP-QPSK modulator is biased as an e-PM, which functions in conjunction with a PS-FBG to form a high-Q OEO, and the other DP-MZM in the DP-QPSK modulator injected by the oscillation signal functions as a frequency multiplier, a microwave phase-coded signal generator or an optical frequency comb generator, respectively, with different signal injection methods. The major advantage of the proposed technique is that both frequency tunability and multi-format signal generation are achieved using a simple and compact system with no RF source. An experiment is performed. A fundamental oscillation signal with a frequency from about 7.5 GHz to 12.5 GHz is generated in the OEO loop, which is used as the reference signals for frequency-doubled and quadrupled signal generation up to 40 GHz, for 8.50 GHz, 12.66 GHz and 17.00 GHz binary phase-coded microwave signal generation, and for five-line optical frequency comb generation.

Funding

National Natural Science Foundation of China (NSFC) (61601297, 61422108); Fundamental Research Funds for Central Universities.